Available online at www.sciencedirect.com

ScienceDirect

journal homepage: www.elsevier.com/locate/he

Electrochemical conversion of CO_2 to methanol using a glassy carbon electrode, modified by Pt@histamine-reduced graphene oxide

Reyhaneh Fazel Zarandi, Behzad Rezaei[*], *Hassan S. Ghaziaskar, Ali Asghar Ensafi*

Department of Chemistry, Isfahan University of Technology, Isfahan, 8415683111, Iran

HIGHLIGHTS

- Pt@histamine-reduced graphene oxide is synthesized by oxidative diazonium reaction.
- The prepared nanocomposite efficiently reduces CO_2 to methanol.
- Histamine stabilizes CO_2 on the electrode surface for the optimized reduction.
- A quite low applied potential is required for CO_2 electrolysis.

GRAPHICAL ABSTRACT

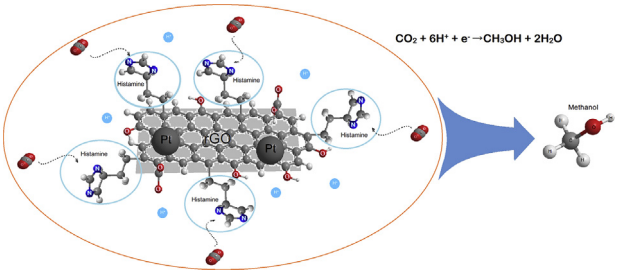

ARTICLE INFO

Article history:
Received 2 June 2019
Received in revised form
26 September 2019
Accepted 30 September 2019
Available online xxx

Keywords:
CO_2 electrochemical reduction
Electrocatalyst
Platinum nanoparticles
Histamine
Reduced graphene oxide plates
Methanol

ABSTRACT

The electrochemical reduction of CO_2 to value-added products is one of the useful approaches to reducing the effects of global climate change. Herein, a novel electrocatalyst consisting of platinum nanoparticles on histamine-reduced graphene oxide plates (Pt@His-rGO) supported by a glassy carbon (GC) substrate for the electrochemical conversion of CO_2 to methanol has been developed. The nanocomposite was optimized in terms of pH, applied potential, CO_2 purging time and platinum loading for the highest current densities and faradaic efficiencies toward methanol production. The best results were obtained in a solution containing KNO_3 0.1 mol L^{-1} at the pH of 2.0, the applied potential of −0.3 V vs Ag/AgCl (KCl_{sat}), CO_2 purging duration of 30 min and Pt loading of 5.17×10^{-7} mol cm^{-2}. The faradaic efficiency of 37% was obtained for methanol production. The prepared nanocomposite requires a lower applied potential and serves as an intermediate stabilizer through the production of methanol.

* *Corresponding author.*
E-mail address: rezaei@cc.iut.ac.ir (B. Rezaei).

https://doi.org/10.1016/j.ijhydene.2019.09.237

Introduction

The increase in the emissions of carbon dioxide, as a compound, has caused a lot of concerns regarding global warming and its devastating effects on the environment in recent years. While there are both natural and human sources of CO_2 emissions, since the industrial revolution, human-related emissions are largely responsible for its increase in the atmosphere [1]. CO_2 emissions have considerably increased in the last decades due to extreme energy consumption, such that the recorded CO_2 concentration in 2014 has been about 400 ppm which has amplified by 25% from its normal amount (280 ppm) before the industrial revolution began in the 18th century [2]. The effects of global climate change are numerous and include drought, flooding, change in seasonal timing events, strong hurricanes, immigration, universal conflicts, etc. [3,4]. The destructive effects of CO_2 are due to its remarkable ability in absorbing the solar IR radiation which should ideally escape from the atmosphere to space, but instead, it is trapped by CO_2 and desorb in the atmosphere as heat [5]. Scientifically, for the reduction of CO_2, there are two possible approaches to reduce the global warming effects. The first option is capturing and storing CO_2 and the second one, which is an interesting attempt, is converting CO_2 to chemical feedstock and fuels. Various techniques, such as thermochemical, chemical, electrochemical, photochemical, photoelectrochemical, and biochemical methods have been established to convert CO_2 to useful products [6–11]. Amongst these techniques, the direct electrochemical reduction of CO_2 to value-added products has been inspected multitudinously due to its simplicity and operating under ambient conditions [12,13]. The products obtained by this conversion method include methane, formate (or formic acid), ethane, ethylene, methanol, ethanol, etc which have been addressed applying various electrochemical conditions considering different operational parameters [10,14–20]. Metal, carbon, polymer, and composite-based electro-catalysts [20–24] have been examined, focusing on the electrochemical conversion of CO_2. Recently, the utilization of metal-organic frameworks [25–27], especially those with the bimetallic compositions [28], has been under the investigation to take advantage of their tunability which increases the selectivity towards one specific product with high faradaic efficiency [29]. However, in some cases, a tiny fraction of a secondary metal can totally poison the CO_2 conversion ability [30,31].

The modification of electrocatalysts could enhance the faradaic and conversion efficiencies of the reduction processes effectively. Recent modification methods in the synthesis of efficient catalysts are designed, for instance, to control the dimensions of nanoparticles with monodispersive configuration [32]. Nowadays, the catalytic effects of nanoparticles can be evaluated more accurately by identifying the active sites of catalysts to optimize the catalytic properties [33]. Amongst the metallic electrocatalysts, Pt nanoparticles have been used for CO_2 conversion. Pt-based electrocatalysts usually convert CO_2 to CO but their behavior could change depending on the electrolyte media which alters the reduction route. According to literature, the mass signals of methanol and formaldehyde have been produced by CO_2 reduction in 0.1 M $HClO_4$ with cathodic potential steps of 0.2 to −0.9 V vs. RHE applied to Pt deposited on an Au substrate [34].

In addition to heterogeneous electrocatalysts used for the electrochemical reduction of CO_2, there are various homogeneous electrocatalysts which are available in different forms such as organic solvents, ionic electrolytes, and metal complexes. Recent studies show that basic heterocyclic organic compounds such as pyridine have an outstanding effect on facilitating the electrochemical CO_2 conversion reaction [9,35]. The pyridinium radical plays a key role in the reduction of the reaction intermediates through a six electron transfer route to the final reduced product such as methanol. Previously, it has been assumed that multiple electron transfers derived from metals were essential to obtain highly reduced compounds. Notably, a small simple organic molecule such as pyridine is realized to be able to reduce various chemicals by sequentially transferring 6 electrons rather than metal-based multi-electron transfer. As a matter of fact, the nitrogen atoms in the conjugated catalyst's molecular structure play the main role during the reduction process [36]. Accordingly, scientists are interested in using nitrogenous heterocyclic compounds and examining their efficiency in electrochemical CO_2 reduction. However, some of these chemicals are toxic and challenging from environmental aspects.

In addition, Graphene oxide (GO) as an improved carbon material, is being used in many applications [37,38], and especially in catalysts [39,40]. GO has been formed by extremely thin layers of interconnected carbon atoms with a lateral size of a few micrometers and thickness of less than 1 nm. Carbon atoms' hybridization angles in GO are 90° and 120° and it contains the oxygen functional groups such as epoxy, hydroxyl, carbonyls and carboxyl [41]. By reducing of GO and changing it to the reduced graphene oxide (rGO), we can change the oxygen content and enhance its chemical properties toward particular purposes such as CO_2 reduction.

Interestingly, the immobilization of generally toxic nitrogenous heterocyclic compounds on the electro-active supports (such as GO) could be an advantage to the environment's safety. One of the attempts for the immobilization of heterocyclic compounds was reported by Ensafi et al.'s study in which rGO was functionalized by adenine and examined for its electrochemical CO_2 reductive abilities [42]. Their results showed a quite high faradaic efficiency for the production of methanol.

Thus, considering the incredible properties of rGO and the selective effects of heterocyclic compounds on CO_2 reduction, one could profit from their collaborative functions via assembling the heterocyclic compounds on rGO which is the main effort at the current work. The novelty of current work is utilizing histamine as a heterocyclic compound with an electron-rich ring to functionalize the rGO and enhance its electroactivity toward the adsorption of CO_2. Furthermore, the electrodeposition of Pt nanoparticles on modified rGO could provide the required hydrogen radicals for the reduction process. This combination may create a suitable nanocomposite for the production of more sophisticated products with high faradaic efficiencies. In this study, to elaborate on the required technical aspects, the effects of pH, applied potential, and the amount of electrodeposited Pt nanoparticles for the desired conversion efficiency have been investigated.

Please cite this article as: Zarandi RF et al., Electrochemical conversion of CO_2 to methanol using a glassy carbon electrode, modified by Pt@histamine-reduced graphene oxide, International Journal of Hydrogen Energy, https://doi.org/10.1016/j.ijhydene.2019.09.237

Experimental

Materials

Graphite powder, KNO_3, KOH, HNO_3, $NaNO_2$, HCl, and H_2SO_4 were provided by Merck. The high purity analytical grade materials such as histamine hydrochloride, K_2PtCl_6 and Fe powder (particle size: <10 μm) were purchased from Sigma-Aldrich. During all experiments, deionized water was used.

Instruments

For electrochemical measurements, a computer-controlled Autolab potentiostat/galvanostat (Model PGSTAT 30) was used. All of the experiments were carried out in an H-shaped electrochemical cell supplied with a platinum rod auxiliary, an Ag/AgCl (KCl saturated) reference and a glassy carbon working electrode (GCE) with an area of 0.196 cm^2 modified by Pt@His-rGO. For the characterization of prepared nanocomposite and the modified electrode, FT-IR spectroscopy (model JASCO 680 plus), energy-dispersive X-ray spectroscopy (EDX) and scanning electron microscopy (SEM) instruments (Model XL30, Philips) were used. For the analysis of products, a gas chromatograph-mass spectrometer (Agilent HP-5973) with an HP-5MS capillary fused silica column was utilized.

Synthesis of GO and rGO

Firstly, GO was prepared using the modified Hummers' method [43]. In brief, 3.0 g of graphite powder and 1.5 g of $NaNO_3$ were added together into 69 mL of concentrated H_2SO_4 and the mixture was kept at 0 °C. Then, 9.0 g of $KMnO_4$ was gradually added to the mixture in order to maintain the reaction temperature below 20 °C. The mixture was heated to 35 °C and mixed for half an hour before the slow addition of 140 mL of water. This process turned the mixture's temperature to less than 100 °C and this temperature was maintained for 10 min and then, the mixture was allowed to cool to room temperature. In the next step, 3 mL of 30% hydrogen peroxide was mixed with 420 mL water and added to GO dispersion to eliminate the excess $KMnO_4$ developing a great amount of heat. After reaching room temperature, the mixture was filtered and washed for several times and dried overnight. For the reduction of GO to rGO, 0.1 g of GO was added in 100 mL of water sonicated for 15 min to finely disperse GO in the mixture and through the procedure, the suspension temperature was kept at 0 °C. Then, $NaBH_4$, as a reducing agent, was added to the dispersed GO mixture so that the weight ratio of $NaBH_4$: GO became 5:1 and after that the suspension was stirred for 24 h. The obtained product was centrifuged and washed with water several times to reach a neutral pH and left at room temperature to dry [44].

Synthesis of histamine-reduce graphene oxide (His-rGO)

To synthesize histamine-reduced graphene oxide, the procedure was similarly followed by a previous report [45], which in brief, a solution containing 0.5 mol L^{-1} of HCl, 0.05 mol L^{-1} of $NaNO_2$ and 0.05 mol L^{-1} of histamine was prepared and kept at 0 °C. It was followed by the addition of 0.5 g Fe powder. In the next step, by adding 0.1 g of the prepared rGO to the mixture and stirring it overnight, the aimed product was obtained and was washed with distilled water and left to dry at room temperature. The proposed mechanism for this procedure is illustrated in Scheme 1. The role of diazonium salt in the first step of the reaction is oxidizing the primary amino group of histamine to transform it into a diazo group. The added Fe powder acts as a reducing agent and donates either one single electron or a pair of them to the diazo group producing the diazo or ethylene radicals, respectively which are both really active and bind covalently to the rGO surface.

Fabrication of the modified GCE

2.0 mg of histamine-reduced graphene oxide was added to 1.0 mL of water and finely dispersed by sonication. Before modifying the GCE as the working electrode, it was polished with alumina powder (0.05 μm) and examined by the Fe probe. After that, 10 μL of the His-rGO mixture was placed on the GCE surface and left at room temperature to dry. Next, platinum nanoparticles were electrodeposited by immersing His-rGO/GCE in a solution of H_2SO_4 (0.5 mol L^{-1})and K_2PtCl_6 (5 mmol L^{-1}) and then, cycling the electrode potential from −0.30 to +1.30 V at 100 mV s^{-1} for appropriate number of times by which eventually a Pt@His-rGO/GCE was fabricated.

CO_2 electrolysis

Prior to any electrochemical procedure, the electrolyte of 0.1 mol L^{-1} KNO_3 was saturated with CO_2 with the flow rate of 10 mL min^{-1} for 30 min in an H-shaped sealed electrochemical cell in which the cathode and anode were separated by Nafion 117 membrane. To ensure that the electrolyte was saturated with carbon dioxide, the titration was performed by NaOH solution at different purging durations, and after half an hour, the concentration of the carbon dioxide was fixed. As a result, the above duration and flow rate for the CO_2 inlet were considered in all of the experiments. With constant CO_2 purging, the solution was electrolyzed for a half an hour using Pt@His-rGO/GCE at different applying conditions. After the electrolysis, the cyclic voltammogram of the final products was obtained considering the highest oxidation peak current. In this study, in addition to the solution pH and applied reduction potential, the amount of the deposited platinum was also optimized.

Results and discussion

Characterization of GO, rGO, His-rGO and Pt@His-rGO/GCE

For functional conformation, the FT-IR analysis of GO, rGO, and His-rGO, which is shown in Fig. 1A, was carried out. It is clear that, for GO, there is a broadband of absorption in the range of 2000–3700 cm^{-1} compared to rGO in the same region. This is due to extensive vibrational modes of O–H and C–H groups. The absorption bands of GO are attributed to C–O, and C–O–C (1047 cm^{-1}), C–C (1581 cm^{-1}) bending, C=O stretching (1736 cm^{-1}) of carboxyl and carbonyl and the

Please cite this article as: Zarandi RF et al., Electrochemical conversion of CO_2 to methanol using a glassy carbon electrode, modified by Pt@histamine-reduced graphene oxide, International Journal of Hydrogen Energy, https://doi.org/10.1016/j.ijhydene.2019.09.237

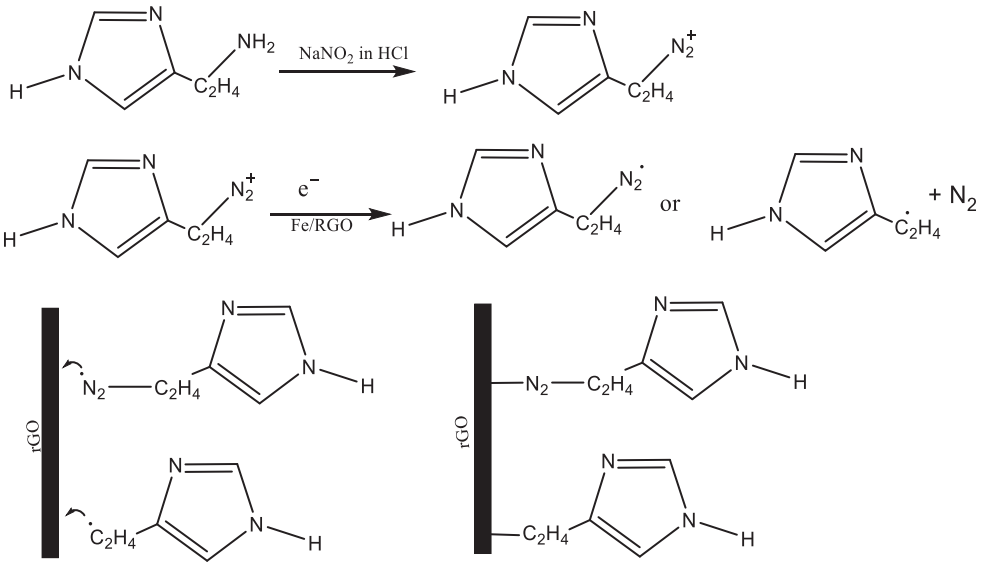

Scheme 1 – The proposed mechanism for histamine bonding to rGO surface.

stretching of O–H (3400 cm^{-1}), confirming the approved previous results for GO synthesis. For the rGO, it seems that despite GO there are no strong peaks related to oxygenated functional groups and only a few vibrational modes including the stretching of C–O–C (1213 cm^{-1}), C=C (1581 cm^{-1}) are observed confirming the adequate procedure of GO reduction to rGO [46]. The FT-IR spectrum of His-rGO shows different absorption bands, such as the out of plane bending of N–H (573 cm^{-1}), the in-plane bending of C–H (746 cm^{-1}), the stretching of C–N (1026 cm^{-1}), N–H of imidazolium ring in-plane bending (1219 cm^{-1}), the ring substitute stretching of C–H (1417 cm^{-1}), and C–H stretching of ring (3180 cm^{-1}). The EDX spectrum shown in Fig. 1B demonstrate the peaks related to Pt and C which are the required evidence for the presence of deposited Pt nanoparticles on rGO sheets. Fig. 1C and D displays the SEM images of the synthesized His-rGO and Pt@His-

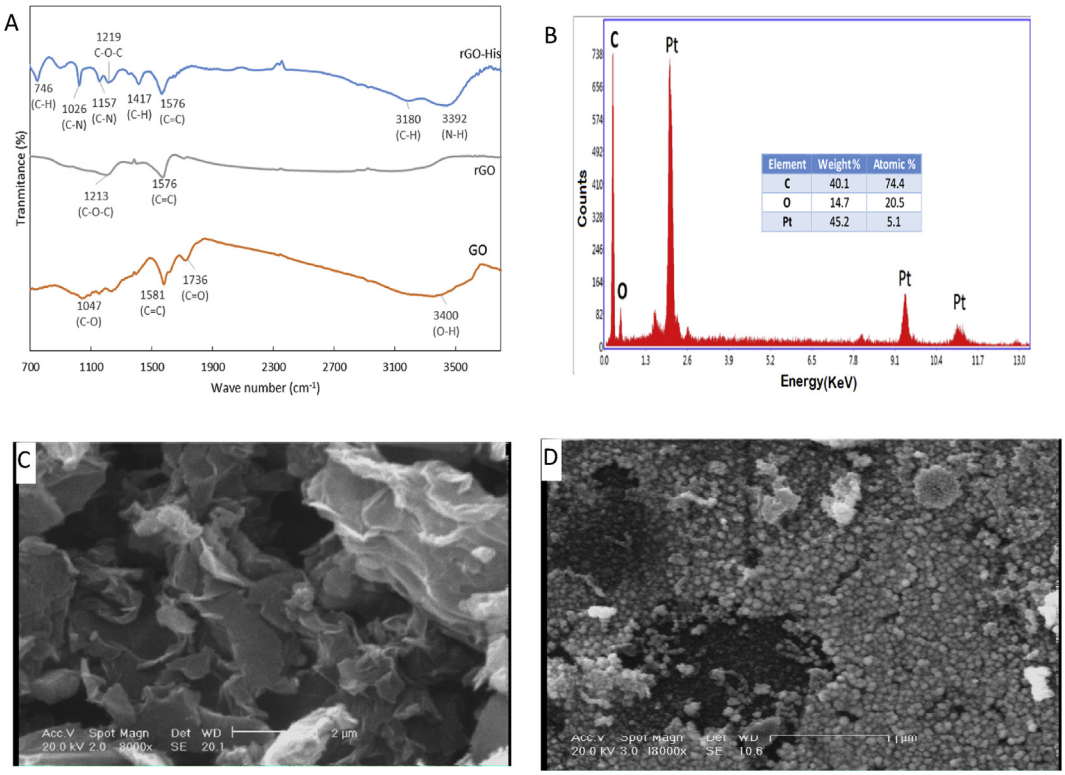

Fig. 1 – (A): FT-IR spectra of GO, rGO, and His-rGO, (B): EDX spectrum of Pt@ His-rGO nanocomposite, (D) and (C): SEM images of His-rGO, and Pt@ His-rGO,respectively.

Please cite this article as: Zarandi RF et al., Electrochemical conversion of CO_2 to methanol using a glassy carbon electrode, modified by Pt@histamine-reduced graphene oxide, International Journal of Hydrogen Energy, https://doi.org/10.1016/j.ijhydene.2019.09.237

rGO nanocomposite, respectively. Pt grains with the size of about 50 nm which are distributed evenly are noticeable in the nanocomposite.

Electrochemical evaluation of the GCE modified electrode

In order to evaluate the applicability of the fabricated electrode for CO_2 electro-reduction, N_2 and CO_2 were initially purged in the separate acidic KNO_3 (0.1 mol L^{-1}) solutions for a few minutes and then, the electrolysis was performed using a GCE modified with Pt@His-rGO. Then, for each solution, the cyclic voltammetry method was applied right after the electrolysis. The results are shown in Fig. 2A. According to curve a in Fig. 2A, it is obvious that no product's peak current has been produced in the solution electrolyzed in the presence of N_2, unlike the voltammogram obtained in the solution electrolyzed in the presence of CO_2 (curve b) which demonstrates an oxidation peak at 0.55. In this study, the main criterion is whether methanol has been produced or not. The appearance of oxidation peak current at the potential of 0.55 V is related to methanol which was examined through the calibration method Fig. S1A (Suplimentary material) and S1B (Suplimentary material). The produced current density includes both faradaic and charge storing Currents. Thus, in the absence of CO_2, the electrocatalyst could slightly behave as an energy storing material. Therefore, a higher current density is not definitely indicative of higher amount of products. Also, the oxidation peaks which appeared at −0.12, −0.05 and 1.0 V are related to Pt(0), Pt(II) and H_2O, respectively and reduction peaks observed at 0.35 and −0.22 V are attributed to Pt(IV) and Pt(II), respectively.

Electrochemical optimization

In the electrochemical reduction of CO_2, the electrolyte pH and applied reduction potential have a considerable influence on the faradaic efficiency of the products. To optimize the pH, 0.1 mol L^{-1} KNO_3 was utilized, as an electrolyte, and the pH was adjusted using HNO_3 or KOH 1.0 mol L^{-1} in the pH range of 1.0–5.0. Then, the voltammograms of solutions with different pH values were recorded and the optimized pH was obtained for the highest peak current (Fig. 2B). The results of this experiment revealed that the optimum pH for the reduction of carbon dioxide is equal to 2.0. Studies show that histamine, as a strong base, has two basic centers of pK_a including 9.4 which is related to amino group hydrogen and 5.8 which is related to the hydrogen-bonded to imidazolium ring nitrogen [47]. As mentioned in the introduction section, pyridine exhibits outstanding behavior in the electrochemical CO_2 reduction. This kind of reaction could be followed by other compounds with structures similar to pyridine. According to a previous research, imidazolium ring may react with CO_2 more strongly than pyridine due to the fact that in its structure there are six electron distributed over 5 ring atoms and the tendency to donate the required electron is increased. Also, it is been found that by analyzing a series of imidazolium derivatives, the existence of C2 proton is essential for imidazole catalysis [10]. Therefore, the nitrogen groups in the structure of histamine are protonated in low pH ranges and the protonation of the histamine imidazolium ring nitrogen at lower pH causes the activation of C2 atom. Thus, it reacts with CO_2 and starts a catalytic pathway toward the production of methanol through the generation of intermediates and complexes. In the absence of histamine, Pt nanoparticles are responsible for CO_2 conversion and, in this case, the main products are CO and H_2 because, firstly, Pt has a great tendency towards adsorbing CO molecules which eventually cover the substrate without further reduction. Pt nanoparticles are also capable of producing hydrogen radicals and excess surface-adsorbed atoms in an acidic environment [9], therefore, the chance of HER increases. However, Shironita et al. [48] investigated the CO_2 electroreduction at a carbon supported Pt (Pt/C) and Pt–Ru (Pt–Ru/C) electrode in a single cell to realize a CH_3OH-based reversible fuel cell. Their attempt for the electroreduction of CO_2 was shown to occur with relatively high faradaic efficiencies. Here, Histamine could play a mediating role to stabilize intermediates and provide them with the appropriate time to interact with hydrogen radicals produced by Pt nanoparticles. The performance mechanism that can be proposed is as shown in Scheme 2.

The mechanism begins with the protonation of imidazolium ring. Then, the obtained imidazolium cation is reduced by $1e^-$ to give an imidazolium radical followed by the release of a hydrogen atom and the generation of an imidazolium

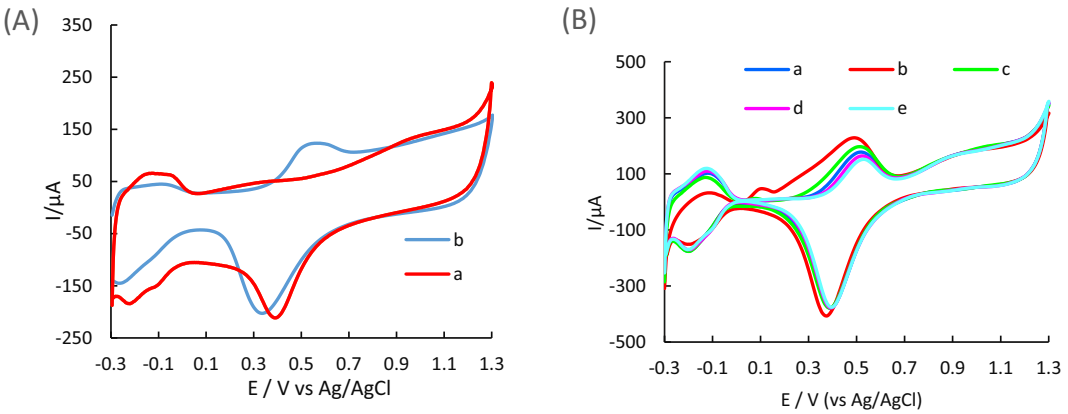

Fig. 2 – (A): The comparison of voltammogram produced after electrolysis in 0.1 mol L^{-1} KNO_3 solution saturated with (a) N_2 and (b) CO_2, (B): Cyclic voltammogram of product in 0.1 mol L^{-1} KNO_3 solution, saturated with CO_2, at pH (a) 1, (b) 2, (c) 3, (d) 4, and (e) 5 after CO_2 electrolysis at −0.3 V (*vs.* Ag/AgCl).

Please cite this article as: Zarandi RF et al., Electrochemical conversion of CO_2 to methanol using a glassy carbon electrode, modified by Pt@histamine-reduced graphene oxide, International Journal of Hydrogen Energy, https://doi.org/10.1016/j.ijhydene.2019.09.237

anion. This anion could show a strong interest to react with CO_2 on C2 carbon and through the protonation a formyl substituent is formed. Further protonation, reduction and dehydration processes through the remaining steps may cause the production of some intermediates such as formic acid and formaldehyde and finally in the last step methanol as the main product is obtained. To distinguish methanol production in the electrolyte solution during the electrolysis, cyclic voltammogram of methanol was recorded. The peak potential of methanol at Pt@His-rGO/GCE appeared at around +0.55 V (*vs.* Ag/AgCl). To optimize the applied reduction potential, a solution of 0.1 mol L^{-1} KNO_3, saturated with carbon dioxide with pH of 2.0, was electrolyzed on Pt@His-rGO/GCE at a constant potential range of 0.00 to −0.50 V (*vs.* Ag/AgCl) for half an hour. After the electrolysis, the cyclic voltammogram of the product was recorded to explore the optimum applied potential based on the highest peak current (Fig. 3A). Using a low range calibration curve, the amount of produced methanol was estimated at the above potential range (Fig. 3B) and the results showed that the applied potential of −0.30 V (*vs.* Ag/AgCl) produced the highest amount of methanol.

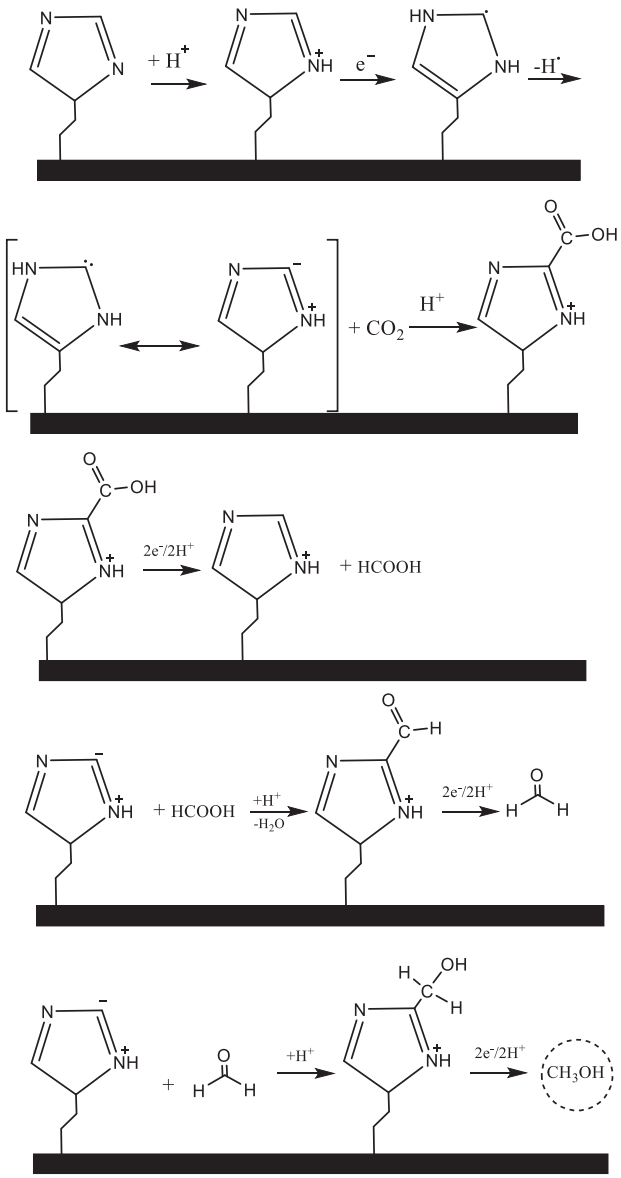

Scheme 2 − The proposed mechanism for electrolysis of CO_2 on the modified GCE.

In the prepared nanocomposite, Pt, with low hydrogen evolution reaction overpotential, plays the main role for proton transfer during methanol production [49], Such that in an acidic solution, it produces enough hydrogen radicals needed for the reduction of CO_2 on a modified Pt@His-rGO/GCE. For this reason, the amount of the optimum platinum content deposited on His-rGO/GCE was controlled by the number of the cycles in the cyclic voltammetry. To obtain the optimum amount of Pt, different amounts of platinum were electrodeposited on the His-rGO/GCE and then, the CO_2 electrolysis was carried on the solution of 0.1 mol L^{-1} KNO_3, saturated with CO_2 at the optimum pH and potential for a half an hour. To obtain the optimum amount of the loaded Pt nanoparticles, the cyclic voltammogram of the product was recorded for the modified electrodes in which Pt nanoparticles were loaded on them for a different number of scans. Considering the highest product's peak current, shown in Fig. 4A–B, the optimum amount of the Pt was 5.17×10^{-7} mol cm^{-2} which was loaded for 50 scans. The amount of the Pt was determined using equation (1) [50],

$$\Gamma = Q/nFA \quad (1)$$

in which, Γ, Q, n, F, and A are the surface excess, the charge under the voltammetric peak for Pt reduction, the number of the transferred electron for the reduction, Faraday constant and the area of the electrode, respectively.

For the electrochemical evaluation of the produced products on the surface of the modified electrodes in CO_2 reduction, a solution of 0.1 mol L^{-1} KNO_3 was saturated with carbon dioxide in the pH of 2.0 and electrolyzed at −0.30 (*vs.* Ag/AgCl) for half an hour on a His-rGO/GCE and Pt@His-rGO/GCE. After the electrolysis, the cyclic voltammogram of the product was recorded to see if any methanol was produced. Fig. 5 showing the cyclic voltammograms of His-rGO/GCE and Pt@His-rGO/GCE in an inert N_2 saturated electrolyte indicates no peak current for the presence of product after the electrolysis and proves that the source of the product is the CO_2 purged into the solution rather than electrocatalyst's carbon source. On the other hand, after the bulk electrolysis in a CO_2 saturated electrolyte, a clear product oxidation peak produced by Pt@His-rGO/GCE is completely obvious in Fig. 5. Another important point to be observed in Fig. 5 is the cyclic voltammogram of Pt@His-rGO/GCE in a solution containing 2.0 mmol L^{-1} methanol with the oxidation peak of methanol at around 0.55 V (vs Ag/AgCl) which is similar to the voltammogram of the CO_2 saturated solution of 0.1 mol L^{-1} KNO_3 electrolyzed in the optimum, so that methanol is the major product of the electrolysis of carbon dioxide in a KNO_3 solution saturated with carbon dioxide on a Pt@His-rGO/GCE. These results substantiate the important role of platinum in the reduction of carbon dioxide to methanol by providing the required hydrogen radicals for the process.

Considering the amount of diffusion controlled current, CO_2 electroreduction time, soluble CO_2 concentration

Please cite this article as: Zarandi RF et al., Electrochemical conversion of CO_2 to methanol using a glassy carbon electrode, modified by Pt@histamine-reduced graphene oxide, International Journal of Hydrogen Energy, https://doi.org/10.1016/j.ijhydene.2019.09.237

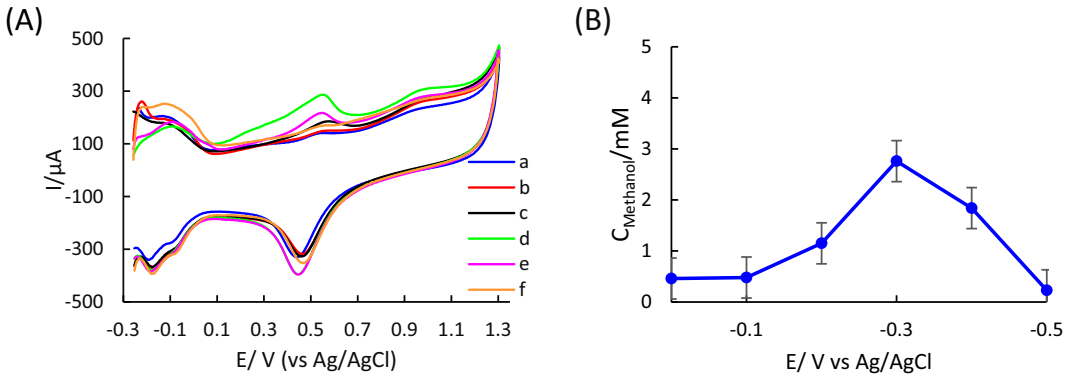

Fig. 3 – (A): Cyclic voltammogram of product in 0.1 mol L^{-1} KNO_3 solution, CO_2 saturated, with the pH of 2 after CO_2 electrolysis at (a) 0.0, (b) −0.1, (c) −0.2, (d) −0.3, (e) −0.4, and (f) −0.5 V (*vs.* Ag/AgCl), (B): The concentration of the produced methanol vs the applied potential.

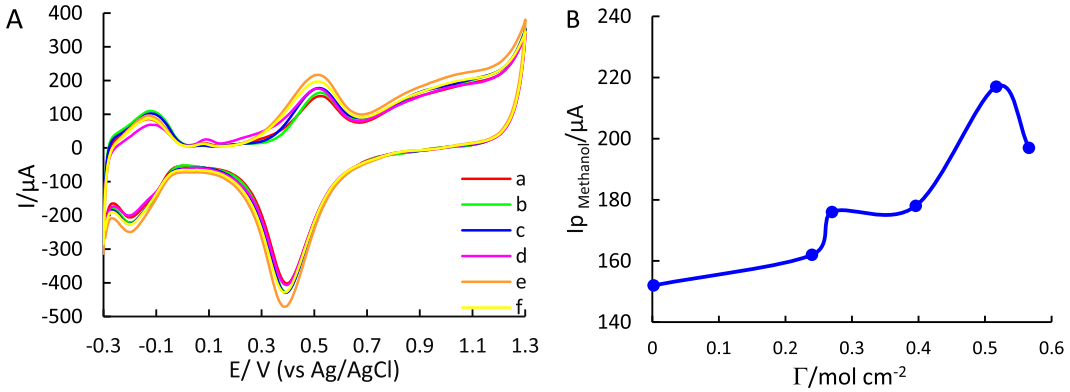

Fig. 4 – (A): Cyclic voltammogram of the product, after the CO_2 electrolysis in the CO_2 saturated 0.1 mol L^{-1} KNO_3 solution at pH of 2 and potential of −0.3 V (*vs.* Ag/AgCl) for (a) 10, (b) 20, (c) 30, (d) 40, (e) 50, and (f) 60 Pt deposition cycles on His-rGO/GCE, (B): Methanol peak current vs Pt surface excess.

(0.033 mol L^{-1}.at ambient conditions), its diffusion coefficient (1.97×10^{-5} cm^2 s^{-1}) [51], and the active surface area of the electrode could readily be calculated from Cottrell equation [52]. Therefore, the approximate active surface area for Pt@His-rGO/GCE is about 0.044 cm^{-2}. In Tables 1–3, the methanol production rate normalized by the catalyst loadings, available reaction areas, and the charge passed through the system are presented in detail. It has been indicated that the increase of catalyst loading reduces the normalized methanol production due to accumulation of Pt@His-rGO sheets and the decline of the active surface area. Also, variation in the geometric surface area of GCE directly affects the available reaction area. Therefore, the normalized methanol production rate decreases by the reduction of the reaction area. The amount of the charge passed through system depends on the applied potential. Although employing high voltages does not lead to the production of higher amounts of methanol, it can increase the formation of gaseous products.

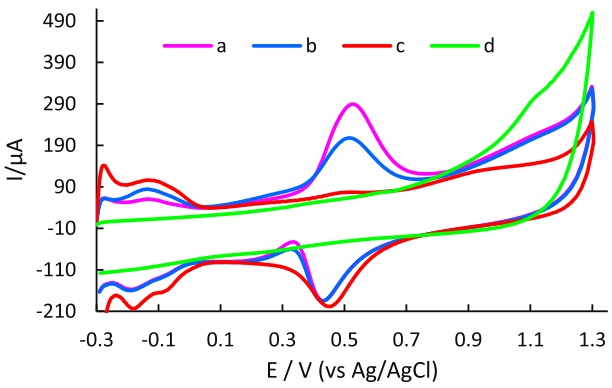

Fig. 5 – Cyclic voltammogram of (a) Pt@His-rGO/GCE in an electrolyte solution consisting of 2.0 mmol L^{-1} methanol, (b) Pt@His-rGO/GCE after 30 min bulk electrolysis in a saturated CO_2 solution, (c) Pt@His-rGO/GCE in a CO_2 free solution and (d) His-rGO/GCE in a CO_2 free solution, at pH 2.0.

Please cite this article as: Zarandi RF et al., Electrochemical conversion of CO_2 to methanol using a glassy carbon electrode, modified by Pt@histamine-reduced graphene oxide, International Journal of Hydrogen Energy, https://doi.org/10.1016/j.ijhydene.2019.09.237

Table 1 – Normalized methanol formation rate by catalyst loadings.

Catalytic loading (μg)	5.0	10	15	20	25
Methanol formation rate (μmol h^{-1})	1.93	2.41	3.18	3.65	3.35
	2.04	2.50	3.19	3.57	3.41
	1.91	2.54	3.24	3.49	3.29
Normalized methanol formation rate (μmol μg_{cat}^{-1} h^{-1})	0.39 ± 0.014	0.248 ± 0.006	0.213 ± 0.002	0.178 ± 0.004	0.134 ± 0.024

Table 2 – Normalized methanol formation rate by available reaction areas of catalysts.

GCE surface area (cm^2)	0.031	0.283	0.785
Available reaction area (cm^2)	0.001	0.015	0.044
Methanol formation rate (μmol h^{-1})	0.081	1.21	3.65
	0.079	1.19	3.57
	0.074	1.23	3.49
Normalized methanol Formation rate (μmol cm^{-2} h^{-1})	78.000 ± 4.000	80.66 ± 1.33	81.14 ± 1.81

Table 3 – Normalized methanol formation rate by the charge passed through the system.

$Q_{theoritical}$[a](C)	1.16	1.98	2.83	3.75	4.43
Methanol formation rate(μmol h^{-1})	0.011	0.74	3.65	2.26	0.61
	0.013	0.77	3.57	2.31	0.55
	0.013	0.68	3.49	2.21	0.48
Normalized methanol Formation rate (μmol C^{-1} h^{-1})	0.0103 ± 0.0008	0.37 ± 0.02	1.26 ± 0.03	0.60 ± 0.01	0.12 ± 0.01

[a] Charge passed through the system.

Analysis of products

CO_2 reduction products in the electrolysis solution were analyzed using cyclic voltammetry and gas chromatography-Mass spectroscopy methods. For the electrochemical approach, a solution of 0.1 mol L^{-1} KNO_3 saturated with CO_2 at pH 2.0 was electrolyzed on Pt@His-rGO/GCE at −0.30 (*vs.* Ag/AgCl) for 16 h and the methanol concentration in the electrolyte solution was determined afterward using a calibration curve via the cyclic voltammetry technique (Fig. 6). Based on the amount of methanol peak current, the amount of methanol produced by the electrolysis of CO_2 was 2.96 mmol L^{-1}.

The other approach for the analysis of the products was gas chromatography-Mass spectroscopy technique which was deployed to separate and identify the concentration of the produced product. As noted in the supplementary material section, the obtained chromatogram (Fig. S2, Supplementary material) shows two main peaks which are attributed to CO_2 and methanol. Moreover, in Fig. S3 (Supplementary material), the spectrum appeared at 2.718 min (Fig. S3A, Supplementary material) was compared with the one recorded on the mass digital library (Fig. S3B, Supplementary material) and proved to be related to methanol. The concentration of the produced methanol was determined to be 2.94 mmol L^{-1}. With regard to the possible formed intermediate, the spectroscopic results showed no information about their presence in the final solution. This is indicative of the limited lifetimes of intermediates.

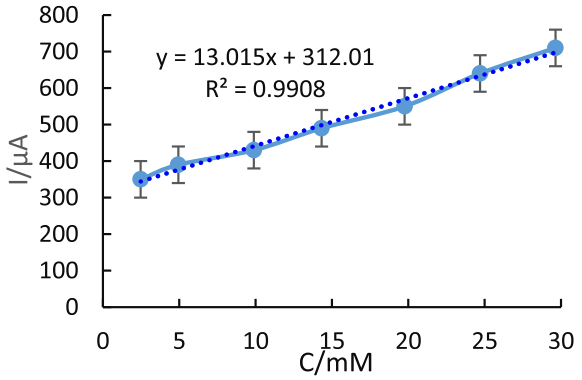

Fig. 6 – The calibration curve produced by the cyclic voltammetry of optimized Pt@His-rGO/GCE in a CO_2-saturated solution to determine methanol concentration based on its peak current.

Employing either of the determination methods, the faradaic efficiency can be calculated using the following equations. According to equation (2), thermodynamically, CO_2 requires receiving 6 electrons to produce methanol:

$$CO_2\,(g) + 6H^+(aq) + 6e^- \rightarrow CH_3OH(aq) + H_2O(l) \quad (2)$$

Considering equations (3)–(5), where I, t, n, F, N_p, Q_{exp}, and Q_{th} are current passed during the electrolysis, time, faradaic constant, the mole number of product, the charge amount consumed for each product and the integrated bulk electrolysis charge, respectively, the faradaic efficiency for the production of methanol from CO_2 was estimated to be 37% in the present study.

$$Q_{th} = I.t \quad (3)$$

$$Q_{exp} = n.F.N_p \quad (4)$$

$$Efficiency\% = Q_{exp} \Big/ Q_{th} \times 100 \quad (5)$$

Moreover, to investigate whether any gaseous product is formed during the electrolysis, a silicone rubber tube was

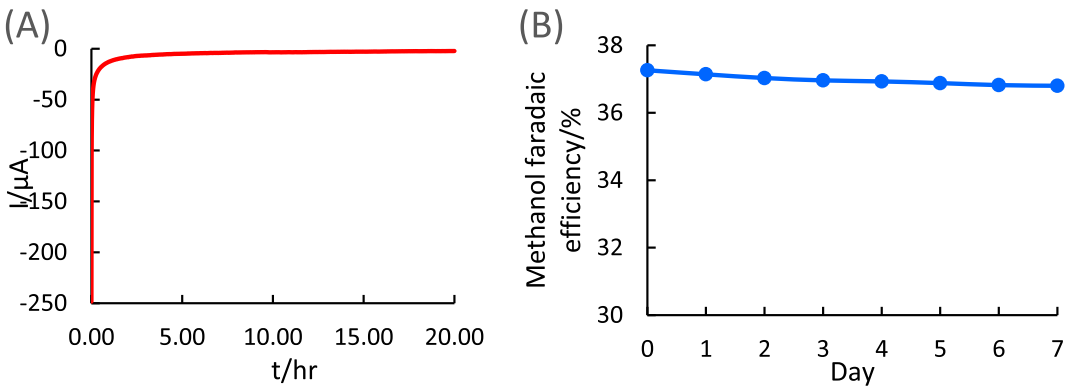

Fig. 7 – (A) Durability test of Pt@His-rGO/GCE at the optimum conditions, (B) Evaluation of methanol faradaic efficiency by daily electrolysis test.

Table 4 – The Comparison between the presented work and some reported experiments in the literature for the electrochemical reduction of CO_2.

Electrocatalyst	Applied potential (V)	FE%	Major product	Ref.
CuO	−1.3 (NHE)	28	Methanol	[53]
Copper nanoparticles supported on carbon black	−1.2 (Ag/AgCl)	~15	CO	[54]
Graphene confined Sn quantum sheets	−1.2 (SCE)	30.0	HCOO−	[55]
Mercaptopteridine	−0.4– −0.9 (Ag/AgCl)	10–23	Methanol	[56]
Cu2O/ZnO-2 mPy	−1.03 (Ag/AgCl)	16.8	Methanol	[35]
Ag	−1.5 (SCE)	81	CO	[57]
Cu	−4.0	37.5	CH_4	[58]
Molecular Fe catalyst	−0.46 (NHE)	90.0	CO	[59]
Organically doped palladium	−0.6 (SCE)	35	Methanol	[60]
Cu2O/ZnO	−1.3 (Ag/AgCl)	17.7	Methanol	[61]
Pt–Ru/C	−0.06 (NHE)	7.5	Methanol	[48]
Boron-doped diamond	−1.3 (Ag/AgCl)	24.3	Methanol	[62]
Pt	−0.55 (NHE)	0.3	Methanol	[63]
Mercaptopteridine	−0.65 (Ag/AgCl)	10–23	Methanol-Formate	[56]
Pd	−0.51	30	Methanol	[64]
$Cu_{63.9}Au_{36.1}$/NCF	–	15.9	Methanol	[65]
		12.0	Ethanol	
LSCM[a]/BCZYZ[b]/Ni	−2.0	~90	CO	[66]
Current work	−0.3 (Ag/AgCl)	37	Methanol	–

[a] $(La_{0.75}Sr_{0.25})_{0.95}Mn_{0.5}Cr_{0.5}O_{3-\delta}$.
[b] $BaCe_{0.5}Zr_{0.3}Y_{0.16}Zn_{0.04}O_{3-\delta}$.

placed on top of the cathode compartment which was connected to a sealed sample bag and after the electrolysis, the collected was analyzed with GC gas analyzer. The results revealed that no valuable product was produced throughout the process due to the application of low potential. Similar findings have been observed in the literature [53].

Pt@His-rGO nanocomposite stability evaluation

The durability of the modified GCE was analyzed by carrying out CO_2 electrolysis in the optimum condition over 20 h. Fig. 7A indicates that current has remained almost constant during the electrolysis which demonstrated the high stability of the Pt@His-rGO/GCE. Furthermore, the faradaic efficiency for the production of methanol was determined after a daily electrolysis test during one week (Fig. 7B) and repeatedly no considerable change was observed in the electroactivity of the modified electrocatalyst for the production of methanol.

A comparison between the results of the new electrocatalyst and the previously-reported electrocatalysts for CO_2 reduction is demonstrated in Table 4 which indicates the higher capability.

Of represented electrocatalyst on the reduction of CO_2 to a more sophisticated product such as methanol.

Conclusion

In this study, a GCE was modified with Pt@His-rGO for the electrochemical reduction of CO_2. The main role in the presented electrocatalyst was played by histamine which led the reduction process through the initial production of formic acid as an intermediate. By the collaboration of Pt nanoparticles with low hydrogen overpotential, the excess surface-adsorbed H atoms available to react with a surface species were provided and a more hydrogenated material such as

Please cite this article as: Zarandi RF et al., Electrochemical conversion of CO_2 to methanol using a glassy carbon electrode, modified by Pt@histamine-reduced graphene oxide, International Journal of Hydrogen Energy, https://doi.org/10.1016/j.ijhydene.2019.09.237

methanol produced. The optimum conditions such as pH, reduction potential and the amount of Pt were determined. The optimum conditions were selected as reduction potential at −0.30 V (*vs.* Ag/AgCl), pH 2.0, and 5.17×10^{-7} mol cm^{-2} Pt. The CO_2 electro-reduction products were analyzed by GC-MS spectroscopy and cyclic voltammetry. The results showed that the only product at Pt@His-rGO/GCE was methanol. From a saturated CO_2 solution during 16 h electrolysis at −0.30 V at pH 2.0, the amount of methanol produced in the electrochemical process was 2.96 mmol L^{-1}. The Faradaic efficiency of methanol production was about 37%. For an electrocatalyst to be commercially viable it is required to obtain a rather high selectivity during the reduction process toward a particular product (especially to more sophisticated products such as alcohols) with a high faradaic efficiency to minimize the necessary separation processes that could dramatically increase the overall capital and operational costs. The presented electrocatalyst has been synthesized and fabricated with rather inexpensive, electroactive, and environmentally friendly materials and demonstrates a very high selectivity toward the production of methanol at ambient temperature and pressure carried by a very simple operational electrochemical procedure.

Acknowledgments

The authors would like to thank the Isfahan University of Technology, Isfahan, Iran for providing the required equipments and financial support of this work.

Appendix A. Supplementary data

Supplementary data to this article can be found online at https://doi.org/10.1016/j.ijhydene.2019.09.237.

REFERENCES

[1] United States Environmental Protection Agency. Overview of greenhouse gases (1990–2017). https://www.epa.gov/ghgemissions/overview-greenhouse-gases; 2017.
[2] Centi G, Perathoner S. Green carbon dioxide: advances in CO_2 utilization. 1st ed. Hoboken, New Jersey: John Wiley & Sons, Inc.; 2014.
[3] IPCC. In: Parry ML, Canziani OF, Palutikof JP, van der Linden PJ, Hanson CE, editors. Climate change 2007: impacts, adaptation and vulnerability. Contribution of working group II to the fourth assessment report of the intergovernmental panel on climate change. Cambridge, UK: Cambridge University Press; 2007. p. 976. https://www.ipcc.ch/site/assets/uploads/2018/03/ar4_wg2_full_report.pdf.
[4] IPCC. In: Stocker TF, Qin D, Plattner GK, Tignor M, Allen SK, Boschung J, et al., editors. Climate change 2013: the physical science basis. Contribution of working group I to the fifth assessment report of the intergovernmental panel on climate change. Cambridge, United Kingdom and New York, NY, USA: Cambridge University Press; 2013. p. 1535. https://www.ipcc.ch/report/ar5/wg1/.
[5] Rothman LS, Gordon IE, Barbe A, Benner DC, Bernath PF, Birk M, et al. The HITRAN 2008 molecular spectroscopic database. J Quant Spectrosc Radiat Transfer 2009;110:533–72. https://doi.org/10.1016/j.jqsrt.2009.02.013.
[6] Inui T, Anpo M, Izui K, Yanagida S, Yamaguchi T. Advances in chemical conversions for mitigating carbon dioxide. 1st ed. Elsevier Science; 1998. p. 114.
[7] Zhang Q, Zhao Q, Liang X, Wang X, Ma FX, Suo BB. Computational studies of electrochemical CO_2 reduction on chalcogen doped Cu_4 cluster. Int J Hydrogen Energy 2018;43:9935–42. https://doi.org/10.1016/j.ijhydene.2018.04.033.
[8] Rao H, Julien B, Robert M. Towards visible-light photochemical CO_2-to-CH_4 conversion in aqueous solutions using sensitized molecular catalysis. J Phys Chem C 2018;122(25):13834–9. https://doi.org/10.1021/acs.jpcc.8b00950.
[9] Cole EB, Lakkaraju PS, Rampulla DM, Morris AJ, Abelev E, Bocarsly AB. Using a one electron shuttle for the multielectron reduction of CO_2 to methanol. J Am Chem Soc 2010;132:11539–51. https://doi.org/10.1021/ja1023496.
[10] Keets KA, Barton E, Morris AJ, Sivasankar N, Teamey K. Analysis of pyridinium catalyzed electrochemical and photoelectrochemical reduction of CO_2: chemistry and economic impact. Indian J Chem 2012;51(9–10):1284–97. http://nopr.niscair.res.in/handle/123456789/14664.
[11] Kirk S, Poust SK. Towards biochemical conversion of CO_2 to higher value chemicals using enzyme design and engineered polyketide synthases. Electronic Theses and Dissertations. UC Berkeley; 2015. https://escholarship.org/uc/item/8vd4s91k.
[12] Whang HS, Lim J, Choi MS, Lee J, Lee H. Heterogeneous catalysts for catalytic CO_2 conversion into value-added chemicals. BMC Chem Eng 2019;7:1–19. https://doi.org/10.1186/s42480-019-0007-7.
[13] Wang H, Leung DYC, Xuan J. Modeling of a microfluidic electrochemical cell for CO_2 utilization and fuel production. Appl Energy 2013;102:1057–62. https://doi.org/10.1016/j.apenergy.2012.06.020.
[14] Kwon Y, Lee J. Formic acid from carbon dioxide on nanolayered electrocatalyst. J Electrocatal 2010;1:108–15. https://doi.org/10.1007/s12678-010-0017-y.
[15] Sheridan LB, Hensley DK, Lavrik NV, Smith SC, Schwartz V, Liang C, et al. Growth and electrochemical characterization of carbon nanospike thin film electrodes. J Electrochem Soc 2014;161:558–63. https://doi.org/10.1149/2.0891409jes.
[16] Qiao J, Liu Y, Hong F, Zhang J. A review of catalysts for the electroreduction of carbon dioxide to produce low-carbon fuels. Chem Soc Rev 2014;43:631–75. https://doi.org/10.1039/c3cs60323g.
[17] Song Y, Peng R, Hensley DK, Bonnesen PV, Liang L, Wu Z, et al. High-selectivity electrochemical conversion of CO_2 to ethanol using a copper nanoparticle/N-doped graphene electrode. Chemistry Sel 2016;1(19):6055–61. https://doi.org/10.1002/slct.201601169.
[18] Peng Y, Wu T, Sun L, Nsanzimana JMV, Fisher AC, Wang X. Selective electrochemical reduction of CO_2 to ethylene on nanopores modified copper electrodes in aqueous solution. ACS Appl Mater Interfaces 2017;9(38):32782–9. https://doi.org/10.1021/acsami.7b10421.
[19] Chen CS, Wan JH, Yeo BS. Electrochemical reduction of carbon dioxide to ethane using nanostructured Cu_2O derived copper catalyst and palladium (II) chloride. J Phys Chem C 2015;119(48):26875–82. https://doi.org/10.1021/acs.jpcc.5b09144.
[20] Albo J, Irabien A. Cu_2O-loaded gas diffusion electrodes for the continuous electrochemical reduction of CO_2 to methanol. J

Catal 2016;343:232–9. https://doi.org/10.1016/j.jcat.2015.11.014.
[21] Hatsukade T, Kuhl KP, Cave ER, Abram DN, Jaramillo TF. Insights into the electrocatalytic reduction of CO_2 on metallic silver surfaces. Phys Chem Chem Phys 2014;16:13814–9. https://doi.org/10.1039/c4cp00692e.
[22] Ye S, Wang R, Wu M, Yuan Y. A review on g-C_3N_4 for photocatalytic water splitting and CO_2 reduction. Appl Surf Sci 2015;358:15–27. https://doi.org/10.1016/j.apsusc.2015.08.173.
[23] Nirmala A, Yi S, Vinoba M, Bhagiyalakshmi M, Hyun D, Yoon Y, et al. Electrochemical reduction of carbon dioxide at low overpotential on a polyaniline/Cu_2O nanocomposite based electrode. Appl Energy 2014;120:85–94. https://doi.org/10.1016/j.apenergy.2014.01.022.
[24] Fan M, Ma C, Lei T, Jung J, Guay D, Qiao J. Aqueous-phase electrochemical reduction of CO_2 based on SnO_2-CuO nanocomposites with improved catalytic activity and selectivity. Catal Today 2018;318:2–9. https://doi.org/10.1016/j.cattod.2017.09.018.
[25] Albo J, Vallejo D, Beobide G, Castillo O, Castaço P. Copper-based metal–organic porous materials for CO_2 electrocatalytic reduction to alcohols. Chem Sustain Chem 2016;10(6):1100–9. https://doi.org/10.1002/cssc.201600693.
[26] Maina JW, Pozo-Gonzalo C, Kong L, Schütz J, Hill M, Dumee LF. Metal organic framework based catalysts for CO_2 conversion. Mater Horiz 2017;4:345–61. https://doi.org/10.1039/C6MH00484A.
[27] Sumida K, Rogow DL, Mason JA, Mcdonald TM, Bloch ED, Herm ZR, et al. Carbon dioxide capture in metal-organic frameworks. Chem Rev 2012;112(2):724–81. https://doi.org/10.1021/cr2003272.
[28] Albo J, Perfecto-irigaray M, Beobide G, Irabien A. Cu/Bi metal-organic framework-based systems for an enhanced electrochemical transformation of CO_2 to alcohols. J CO_2 Utilisation 2019;33:157–65. https://doi.org/10.1016/j.jcou.2019.05.025.
[29] Johnson NJ, Huang A, He J, Berlinguette CP. Electrocatalytic alloys for CO_2 reduction. Chem Sustain Chem 2018;11:48–57. https://doi.org/10.1002/cssc.201701825.
[30] Wuttig A, Surendranath Y. Impurity ion complexation enhances carbon dioxide reduction catalysis. ACS Catal 2015;57:4479–84. https://doi.org/10.1021/acscatal.5b00808.
[31] Hori Y. Electrochemical CO_2 Reduction on metal electrodes. In: Vayenas CG, White RE, Gamboa-Aldeco ME, editors. Modern aspects of electrochemistry, vol. 42. New York: Springer; 2008. p. 89–189.
[32] Li Q, Sun S. Recent advances in the organic solution phase synthesis of metal nanoparticles and their electrocatalysis for energy conversion reactions. Nano Energy 2016;29:178–97. https://doi.org/10.1016/j.nanoen.2016.02.030.
[33] Zhu W, Zhang Y, Zhang H, Lv H, Michalsky R, Peterson AA, et al. Active and selective conversion of CO_2 to CO on ultrathin au nanowires active and selective conversion of CO_2 to CO on ultrathin au nanowires. J Am Chem Soc 2014;136:16132–5. https://doi.org/10.1021/ja5095099.
[34] Brisard GM, Camargo APM, Nart FC, Iwasita T. On-line mass spectrometry investigation of the reduction of carbon dioxide in acidic media on polycrystalline Pt. Electrochem Commun 2001;3(11):603–7. https://doi.org/10.1016/S1388-2481(01)00223-5.
[35] Albo J, Beobide G, Castano P, Irabien A. Methanol electrosynthesis from CO_2 at Cu_2O/ZnO prompted by pyridine-based aqueous solutions. Biochem Pharmacol 2017;18:164–72. https://doi.org/10.1016/j.jcou.2017.02.003.
[36] Bian Z, Sumi K, Furue M, Sato S, Koike K, Ishitani O. A novel tripodal ligand, tris[(4′-methyl-2,2′-bipyridyl-4-yl)methyl] carbinol and its trinuclear Ru II/Re I mixed-metal complexes: synthesis, emission properties, and photocatalytic CO_2 reduction. Inorg Chem 2008;47(23):10801–3. https://doi.org/10.1021/ic801527y.
[37] Eda BG, Chhowalla M. Chemically derived graphene oxide : towards large-area thin-film electronics and optoelectronics. Adv Mater 2010;22:2392–415. https://doi.org/10.1002/adma.200903689.
[38] Tang L, Chang H, Liu Y, Li J. Duplex DNA/graphene oxide biointerface : from fundamental understanding to specific enzymatic effects. Adv Funct Mater 2012;1–6. https://doi.org/10.1002/adfm.201102892.
[39] Wang J, Zhang X, Wang Z, Wang L, Zhang Y. Rhodium–nickel nanoparticles grown on graphene as highly efficient catalyst for complete decomposition of hydrous hydrazine at room temperature for chemical hydrogen storage. Energy Environ Sci 2012;5:6885–8. https://doi.org/10.1039/c2ee03344e.
[40] Wu Z, Yang S, Sun Y, Parvez K, Feng X. 3D nitrogen-doped graphene aerogel-supported Fe_3O_4 nanoparticles as efficient electrocatalysts for the oxygen reduction reaction. J Am Chem Soc 2012;134:9082–5. https://doi.org/10.1021/ja3030565.
[41] Shenoy VB. Chemically derived graphene oxide. Nat Chem 2010;2:581–7. https://doi.org/10.1038/nchem.686.
[42] Alinajafi HA, Ensafi AA, Rezaei B. Reduction of carbon dioxide to methanol on the surface of adenine functionalized reduced graphene oxide at a low potential. Int J Hydrogen Energy 2018;43:23262–74. https://doi.org/10.1016/j.ijhydene.2018.10.188.
[43] Xu Y, Bai H, Lu G, Li C, Shi G. Flexible graphene films via the filtration of water-soluble noncovalent functionalized graphene sheets. J Am Chem Soc 2008;130:5856–7. https://doi.org/10.1021/ja800745y.
[44] Ensafi AA, Jafari-Asl M, Rezaei B. Pyridine-functionalized graphene oxide, an efficient metal free electrocatalyst for oxygen reduction reaction. Electrochim Acta 2016;194:95–103. https://doi.org/10.1016/j.electacta.2016.01.221.
[45] Zeb G, Gaskell P, Le XT, Xiao X, Szkopek T, Cerruti M. Decoration of graphitic surfaces with Sn nanoparticles through surface functionalization using diazonium chemistry. Langmuir 2012;28(36):13042–50. https://doi.org/10.1021/la302162c.
[46] Ensafi AA, Jafari-Asl M, Nabiyan A, Rezaei B, Dinari M. Hydrogen storage in hybrid of layered double hydroxides/reduced graphene oxide using spillover mechanism. Energy 2016;99:103–14. https://doi.org/10.1016/j.energy.2016.01.042.
[47] Paiva TB, Tominaga M, Paiva ACM. Ionization of histamine, N-acetyl histamine, and their iodinated derivatives. J Med Chem 1970;13:689–92. https://doi.org/10.1021/jm00298a025.
[48] Shironita S, Karasuda K, Sato K, Umeda M. Methanol generation by CO_2 reduction at a Pt-Ru/C electrocatalyst using a membrane electrode assembly. J Power Sources 2013;240:404–10. https://doi.org/10.1016/j.jpowsour.2013.04.034.
[49] Ensafi AA, Heydari-Soureshjani E, Jafari-Asl M, Rezaei B. Polyoxometalate-decorated graphene nanosheets and carbon nanotubes, powerful electrocatalysts for hydrogen evolution reaction. Carbon 2016;99:398–406. https://doi.org/10.1016/j.carbon.2015.12.045.
[50] Ensafi AA, Alinajafi HA, Rezaei B. Pt-modified nitrogen doped reduced graphene oxide: a powerful electrocatalyst for direct CO_2 reduction to methanol. J Electroanal Chem 2016;783:82–9. https://doi.org/10.1016/j.jelechem.2016.11.047.
[51] Frank MJW, Kuipers JAM, Swaaij WPM. Diffusion coefficients and viscosities of CO_2+H_2O, CO_2+CH_3OH, NH_3+H_2O, and NH_3+CH_3OH liquid mixtures. J Chem Eng Data 1996;41:297–302. https://doi.org/10.1021/je950157k.

Please cite this article as: Zarandi RF et al., Electrochemical conversion of CO_2 to methanol using a glassy carbon electrode, modified by Pt@histamine-reduced graphene oxide, International Journal of Hydrogen Energy, https://doi.org/10.1016/j.ijhydene.2019.09.237

[52] Trasattia S, Petriib OA. Real surface area measurements in electrochemistry. J Electroanal Chem 1992;327:353–76. https://doi.org/10.1016/0022-0728(92)80162-W.

[53] Le M, Ren M, Zhang Z, Sprunger PT, Kurtz RL, Flake JC. Electrochemical reduction of CO_2 to CH_3OH at copper oxide surfaces. J Electrochem Soc 2011;158:E45–9. https://doi.org/10.1149/1.3561636.

[54] Baturina OA, Lu Q, Padilla MA, Xin L, Li W, Serov A, et al. CO_2 electroreduction to methane and ethene on carbon-supported Cu nanoparticles. ACS Catal 2014;10:3682–95. https://doi.org/10.1021/cs500537y.

[55] Lei F, Liu W, Sun Y, Xu J, Liu K, Liang L, et al. Metallic tin quantum sheets confined in graphene toward high-efficiency carbon dioxide electroreduction. Nat Commun 2016;7:1–8. https://doi.org/10.1038/ncomms12697.

[56] Xiang D, Magana D, Dyer RB, States U. CO_2 reduction catalyzed by mercaptopteridine on glassy carbon. J Am Chem Soc 2014;136:14007–10. https://doi.org/10.1021/ja5081103.

[57] Ham YS, Kim MJ, Lim T, Kim DK, Kim SK, Kim JJ. Direct formation of dendritic Ag catalyst on a gas diffusion layer for electrochemical CO_2 reduction to CO and H_2. Int J Hydrogen Energy 2018;43:11315–25. https://doi.org/10.1016/j.ijhydene.2017.12.067.

[58] Murugananthan M, Kumaravel M, Katsumata H, Suzuki T, Kaneco S. Electrochemical reduction of CO_2 using Cu electrode in methanol/$LiClO_4$ electrolyte. Int J Hydrogen Energy 2015;40:6740–4. https://doi.org/10.1016/j.ijhydene.2015.04.006.

[59] Talanquer V, Oxtoby D, Islam MF, Zhang J, Collings PJ, Yodh AG, et al. A local proton source enhances CO_2 electroreduction to CO by a molecular Fe catalyst. Science 2012;338:90–4. https://doi.org/10.1126/science.1224581.

[60] Yang HP, Qin S, Wang H, Lu JX. Organically doped palladium: a highly efficient catalyst for electroreduction of CO_2 to methanol. Green Chem 2015;17:5144–8. https://doi.org/10.1039/c5gc01504a.

[61] Albo J, Saez A, Solla-Gullon J, Montiel V, Irabien A. Production of methanol from CO_2 electroreduction at Cu_2O and Cu_2O/ZnO-based electrodes in aqueous solution. Appl Catal B Environ 2015;176–177:709–17. https://doi.org/10.1016/j.apcatb.2015.04.055.

[62] Jiwanti PK, Natsui K, Nakata K, Einaga Y. Selective production of methanol by the electrochemical reduction of CO_2 on boron-doped diamond electrodes in aqueous ammonia solution. RSC Adv 2016;6:102214–7. https://doi.org/10.1039/c6ra20466j.

[63] Costentin C, Canales JC, Haddou B, Savéant JM. Erratum: electrochemistry of acids on platinum. Application to the reduction of carbon dioxide in the presence of pyridinium ion in water. J Am Chem Soc 2014;136:17689. https://doi.org/10.1021/ja509820z.

[64] Seshadri G, Lin C, Bocarsly AB. A new homogeneous electrocatalyst for the reduction of carbon dioxide to methanol at low overpotential. J Electroanal Chem 1994;372:145–50. https://doi.org/10.1016/0022-0728(94)03300-5.

[65] Jia F, Yu X, Zhang L. Enhanced selectivity for the electrochemical reduction of CO_2 to alcohols in aqueous solution with nanostructured Cu-Au alloy as catalyst. J Power Sources 2014;252:85–9. https://doi.org/10.1016/j.jpowsour.2013.12.002.

[66] Wu G, Xie K, Wu Y, Yao W, Zhou J. Electrochemical conversion of H_2O/CO_2 to fuel in a proton-conducting solid oxide electrolyser. J Power Sources 2013;232:187–92. https://doi.org/10.1016/j.jpowsour.2013.01.039.

Please cite this article as: Zarandi RF et al., Electrochemical conversion of CO_2 to methanol using a glassy carbon electrode, modified by Pt@histamine-reduced graphene oxide, International Journal of Hydrogen Energy, https://doi.org/10.1016/j.ijhydene.2019.09.237